Geophysical Research Letters

RESEARCH LETTER
10.1029/2018GL081166

Detecting Signals of Large-Scale Climate Phenomena in Discharge and Nutrient Loads in the Mississippi-Atchafalaya River Basin

A. P. Smits[1,2], C. M. Ruffing[3,4], T. V. Royer[5], A. P. Appling[6], N. A. Griffiths[7], R. Bellmore[8], M. D. Scheuerell[9], T. K. Harms[10], and J. B. Jones[10]

[1]School of Aquatic and Fisheries Sciences, University of Washington, St. Louis, Missouri, USA, [2]Now at Environmental Science and Policy, University of California, Davis, California, USA, [3]Institute of Arctic Biology, University of Alaska Fairbanks, Fairbanks, Alaska, USA, [4]Now at Department of Forest and Conservation Sciences, University of British Columbia, Vancouver, British Columbia, Canada, [5]School of Public and Environmental Affairs, Indiana University, Bloomington, Bloomington, Indiana, USA, [6]Data Science Branch, Integrated Information Dissemination Division, U.S. Geological Survey, USGS Arizona Water Science Center, Tucson, Arizona, USA, [7]Environmental Sciences Division and Climate Change Science Institute, Oak Ridge National Laboratory, Oak Ridge, Tennessee, USA, [8]Southeast Alaska Watershed Coalition, Juneau, Alaska, USA, [9]Fish Ecology Division, Northwest Fisheries Science Center, National Marine Fisheries Service, National Oceanic and Atmospheric Administration, Seattle, Washington, USA, [10]Institute of Arctic Biology and Department of Biology and Wildlife, University of Alaska Fairbanks, Fairbanks, Alaska, USA

Key Points:
- Significant signals of large-scale climate phenomena appear in N loads but not discharge, SiO_2, or P loads in the Mississippi River Basin at multiple spatial scales
- Effects of climate variables differ among nutrients (N, P, SiO_2) and nutrient forms (nitrate, ammonium)
- Climate-driven processes independent of river flow contribute to temporal variation in nutrient loads within the Mississippi River Basin

Supporting Information:
- Supporting Information S1

Correspondence to:
A. P. Smits,
asmits@ucdavis.edu

Citation:
Smits, A. P., Ruffing, C. M., Royer, T. V., Appling, A. P., Griffiths, N. A., Bellmore, R., et al. (2019). Detecting signals of large-scale climate phenomena in discharge and nutrient loads in the Mississippi-Atchafalaya River basin. *Geophysical Research Letters*, *46*, 3791–3801. https://doi.org/10.1029/2018GL081166

Received 31 OCT 2018
Accepted 9 MAR 2019
Accepted article online 18 MAR 2019
Published online 3 APR 2019

Abstract Agricultural runoff from the Mississippi-Atchafalaya River Basin delivers nitrogen (N) and phosphorus (P) to the Gulf of Mexico, causing hypoxia, and climate drives interannual variation in nutrient loads. Climate phenomena such as El Niño–Southern Oscillation may influence nutrient export through effects on river flow, nutrient uptake, or biogeochemical transformation, but landscape variation at smaller spatial scales can mask climate signals in load or discharge time series within large river networks. We used multivariate autoregressive state-space modeling to investigate climate signals in the long-term record (1979–2014) of discharge, N, P, and SiO_2 loads at three nested spatial scales within the Mississippi-Atchafalaya River Basin. We detected significant signals of El Niño–Southern Oscillation and land-surface temperature anomalies in N loads but not discharge, SiO_2, or P, suggesting that large-scale climate phenomena contribute to interannual variation in nutrient loads through biogeochemical mechanisms beyond simple discharge-load relationships.

Plain Language Summary Runoff of excess nutrients from crop fertilizers applied throughout the Mississippi-Atchafalaya River Basin, particularly nitrogen (N) and phosphorus (P), pollute freshwater and coastal ecosystems such as the Gulf of Mexico. Though agriculture is the main source, year-to-year variation in the size of nutrient loads is largely controlled by precipitation and river flow, which mobilize nutrients from the landscape. Additional climate variables, such as temperature, influence nutrient loads by controlling rates of nutrient uptake or transformation by plants, algae, and microbes, but these processes may be difficult to detect in a nearly continental-scale river network with heterogeneous subbasins. We identified signals of multiple large-scale climate phenomena in the long-term record (1979–2014) of nutrient loads from the Mississippi River and its major tributaries. Climate effects on nutrient loads, particularly N, were different and often stronger than on river flow, indicating that long-term patterns in nutrient loads were influenced by processes beyond simple precipitation-driven runoff. Variable effects of climate on nutrient export present challenges for reducing nutrient loads to the Mississippi River and Gulf of Mexico. Adjustments to targeted reductions may be needed as global and regional climates change.

1. Introduction

Nutrient loading from the Mississippi-Atchafalaya River Basin (MARB) leads to the formation of a seasonal hypoxic zone in the northern Gulf of Mexico (Rabalais et al., 2002). The size of the hypoxic zone is controlled by the load of nitrogen (N) delivered to the Gulf by the Mississippi and Atchafalaya Rivers (Turner et al., 2012). Agricultural runoff is the major contributor to N and phosphorus (P) loads delivered to the Gulf, with the upper Mississippi and Ohio River basins representing the largest source areas (Dale et al., 2010). Fertilizer inputs to the MARB stabilized in the late 1980s, and interannual variation in N and P loads is

now driven largely by precipitation and runoff within agricultural regions (Donner & Scavia, 2007; Sinha et al., 2017).

Beyond driving runoff, climate variables such as temperature and precipitation influence nutrient-use efficiency by plants and immobilization of nutrients by soil microorganisms. Nitrogen concentrations in streams and small rivers decline during the growing season due to plant uptake (Alexander et al., 2007), and denitrification in soil reduces nitrate runoff and differs widely between wet and dry years (Gentry et al., 2009). In general, the amount and form of N or P available for runoff is affected by biogeochemical processes, both in the soil and during riverine transport, that are temperature or moisture (redox) dependent. Not well understood, however, is the extent to which these biogeochemical processes impart a climate signal on nutrient loads at the spatial scale of the MARB and its major tributaries.

Large-scale climate phenomena such as El Niño–Southern Oscillation (ENSO) and the North Atlantic Oscillation (NAO) likely influence nutrient loads through effects on precipitation patterns and river flows in agricultural regions of the MARB. Riverine nutrient fluxes are greatest during floods (Royer et al., 2006), and extreme precipitation is a strong predictor of N loads (Sinha & Michalak, 2016), but the influence of ENSO or NAO on flood frequency in the MARB remains unclear (Archfield et al., 2016). However, the potential influence of large-scale climate patterns on nutrient loads may extend beyond runoff and flow, and could vary among nutrients and nutrient forms, due to differences in source areas, mobility, and biogeochemical processing during riverine transport (Alexander et al., 2008). Thus, detecting a signal of large-scale climate phenomena within nutrient load time series requires consideration of both flow-driven and flow-independent drivers of nutrient loads.

Spatial heterogeneity within the MARB complicates understanding of climate effects on nutrient processing and export. Climate signals in discharge and nutrient loads can be modified by land cover and artificial drainage within watersheds (Frans et al., 2013), and thus may be inconsistent across spatial scales within the MARB (Rice & Emanuel, 2017). For example, ENSO affects temperature, precipitation, and water balance regionally across the MARB, but has no discernable effect on total discharge to the Gulf of Mexico (Munoz & Dee, 2017; Twine et al., 2005). Landscape characteristics such as soil water storage can further obscure climate signals by triggering lagged responses in discharge and nutrient loads (Chen & Kumar, 2002). Given the degree of spatial heterogeneity and potential asynchrony in climate responses at the scale of the MARB, we expect that climate signals in discharge and material transport may emerge only at regional spatial scales.

We investigated climate-driven patterns in the long-term record (1979–2014) of annual discharge and nutrient loads in the MARB. We applied multivariate autoregressive state-space (MARSS) models to time series of discharge, nitrate, ammonium, total N, total P, and silica loads to assess correlations with climate variables. Rather than building predictive models of nutrient loads, we focused on two sets of hypotheses, the first regarding how climate variables influence discharge and the different nutrients and the second regarding how variation within and among spatial scales mediates or obscures these relationships.

Our first prediction (Hypothesis 1A) was that signals of large-scale climate phenomena would be evident in discharge and nutrient load records, but that climate effects would vary among nutrients. We expected that climate effects, especially those deriving from changes in precipitation and runoff, would be strongest among discharge and the mobile solutes, nitrate, and silica. We expected total P and ammonium loads to be less directly tied to continental-scale climate phenomena because of variable and indirect effects of plant or algal uptake, biogeochemical processing, and retention in soils or sediments. While large-scale climate phenomena can influence regional climate patterns, we predicted that proximate climatic conditions would have a stronger relationship with nutrient loads and discharge at all spatial scales (Hypothesis 1B).

Our second set of hypotheses concerns detection of climate signals at three spatial scales: (1) the entirety of the MARB (MARB scale), (2) four major tributaries within the MARB (subbasin scale), and (3) 13 nonnested watersheds distributed across the MARB (watershed scale; Figure 1). Large rivers are sensitive to disturbances within their watersheds, although effects of regional or smaller-scale disturbances are not always observed further down the river network (McCluney et al., 2014). We expected to detect site-specific statistical relationships between continental-scale climate variables and nutrient loads at the subbasin and

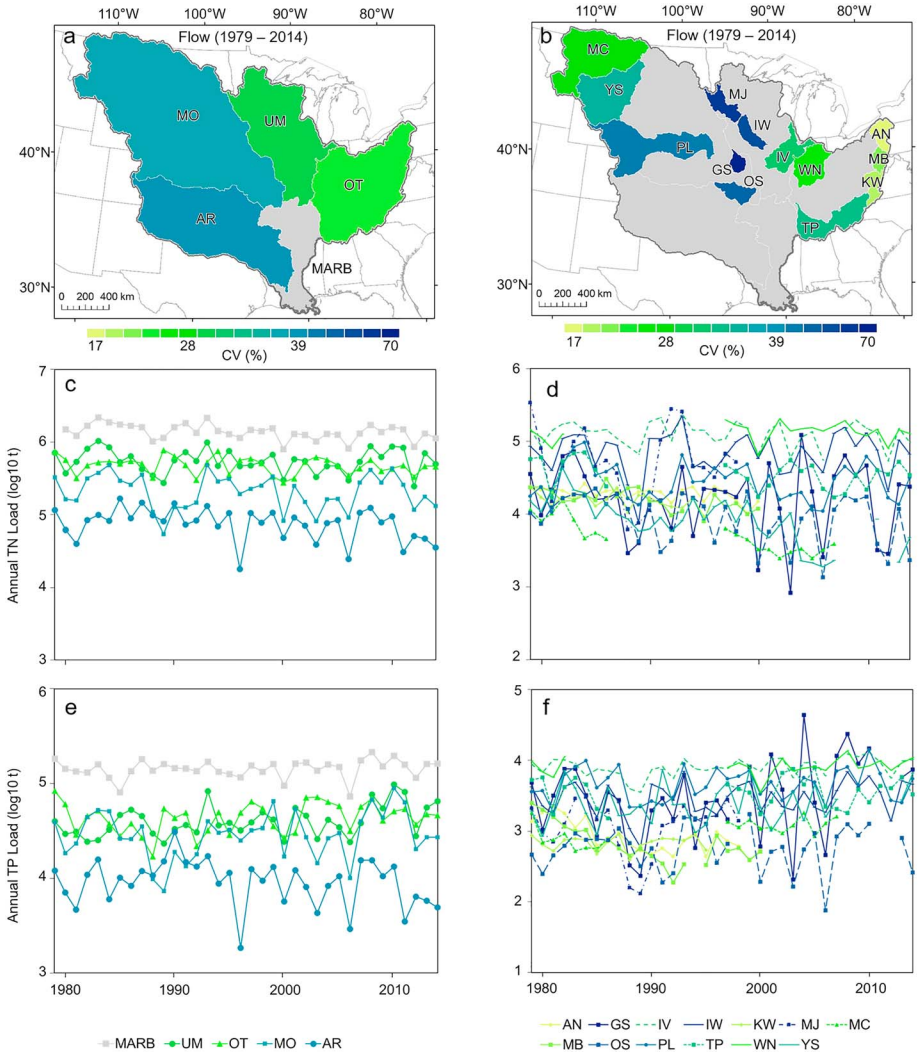

Figure 1. Coefficient of variation in annual discharge at the (a) subbasin and (b) watershed scales and time series of total nitrogen (TN) and phosphorous (TP) loads in metric tons at the MARB, (c and e) subbasin, and (d and f) watershed scales. Abbreviations for study watersheds are reported in the supporting information. The *y* axes in (c)–(f) are on a logarithmic scale.

watershed scales due to variation in catchment characteristics and land use, as well as independent temporal dynamics among sites (Hypothesis 2A). We hypothesized that variable climate responses at the watershed scale would diminish signals of continental-scale climate phenomena at the MARB and subbasin scales (Hypothesis 2B).

2. Data and Methods

2.1. Study Area

The basins included in this study are hierarchically arranged across three spatial scales (Figure 1): the entire MARB, four major tributary subbasins, and 13 individual watersheds within three of the four major subbasins. The MARB drains approximately 3,210,000 km^2 while the 13 smaller watersheds drain areas ranging from 18,000 to 250,000 km^2 (Table S1). Average annual temperature increases from north to south and annual precipitation increases from west to east. Land cover across the MARB is predominantly grass and shrubland in the west, cultivated cropland (i.e., maize, soybean, wheat) in the central portions of the basin, and forest in the east.

2.2. Discharge and Nutrient Loads

We obtained time series of average annual discharge (m^3/s) and total annual nutrient loads (metric tons) from the U.S. Geological Survey (USGS) for each of the basins (Table S2; USGS, 2016). The nutrient forms used in this analysis include total nitrogen (total N; Figures 1c and 1d), nitrate (NO_3^-), ammonium (NH_4^+), total phosphorus (total P; Figures 1e and 1f), and silica (SiO_2). Sites were selected to ensure a sufficient period of record for time series modeling (preferably >20 years; Table S2). Nutrient loads for each water year were calculated by regression on discharge, time, and season using the USGS LOAD ESTimator (LOADEST) software; a five-year moving window was used to calibrate the model in each year, and model form was allowed to vary by year to ensure goodness of fit with observed nutrient concentrations (Aulenbach, 2013; Lee et al., 2017; Runkel et al., 2004; Text S1).

Watershed boundaries were delineated using 30-m digital elevation models from the National Elevation Dataset (USGS, 2009), in ArcGIS (ESRI, 2016). Watershed areas were calculated based on associated USGS gage locations.

2.3. Climate and Agricultural Data

The continental-scale climate drivers included in the analysis were the Multivariate El Niño–Southern Oscillation Index (MEI), the North Atlantic Oscillation Index (NAO), and the Northern Hemisphere Land-Surface Air Temperature Anomaly (SAT; Figure S1). The MEI integrates six variables describing air pressure, wind, and temperature conditions over the Pacific Ocean and is used to monitor the cyclic variability associated with the El Niño–Southern Oscillation (ENSO). Negative values indicate cold La Niña years while positive values indicate warm El Niño years. In this analysis, the MEI was defined as the maximum values from 12 sliding two-month periods each year (NOAA, 2016b). The NAO Index tracks pressure systems over the Atlantic Ocean and describes the strength of westerlies and the intensity of weather systems that influence the eastern United States and western Europe (Hurrell North Atlantic Oscillation (NAO) Index (PC-Based), 2016). The SAT describes the annual mean land surface air temperature relative to the average temperature between 1951 and 1980 for the northern hemisphere (Hansen et al., 2001; NASA, 2016).

Average annual temperature, total annual precipitation, and Palmer Drought Severity Index (PDSI) were chosen to represent yearly climatic variability at the watershed scale (Figure S2). The PDSI describes meteorological drought conditions through parameters reflecting cumulative moisture supply and demand. The original data are reported at monthly time steps by climate division (NOAA, 2016a; Vose et al., 2014). We averaged (temperature and PDSI) or summed (precipitation) values by calendar year for each climate division. Watershed boundaries were used to calculate area-weighted averages for temperature, precipitation, and PDSI for the climate divisions falling within each study watershed. This approach has been used successfully to derive watershed-specific climatic characteristics (Räsänen et al., 2013).

We included an agricultural covariate for comparison to the explanatory power of the climate variables in the nutrient models. Maize and wheat are the predominant nitrogen-fertilized crops in the MARB, and the acres of maize and wheat planted in each county are reported by the National Agricultural Statistics Service (USDA, 2016). We included the annual sum of maize and wheat acres planted in each basin as a proxy for fertilizer input in MARSS models.

2.4. Statistical Methods

We used MARSS models to quantify (1) interannual dynamics in nutrient loads, (2) relationships between climate variables and discharge and nutrient loads, and (3) to determine how these relationships varied across spatial scales and multiple sites within a spatial scale. The MARSS framework is a powerful way to evaluate hypotheses about synchrony among multiple time series (Jorgensen et al., 2016; Ohlberger et al., 2016), and to partition variance in time series data between observation error and environmental stochasticity.

MARSS models are described by two parts. The first, a process model, describes changes in the true, but unobserved, states of nature over time:

$$\mathbf{x}_t = \mathbf{B}\mathbf{x}_{t-1} + \mathbf{C}\mathbf{c}_{t-h} + \mathbf{w}_t \quad (1)$$

$\mathbf{x}_t$ is a $j \times 1$ vector of nutrient loads or discharges in year t for each of the basins; j varies for each of our analyses. The diagonal elements of the $j \times j$ matrix $\mathbf{B}$ determine the degree of mean-reversion of each state

process. The $j \times k$ matrix $\mathbf{C}$ contains the effects of external drivers (climate variables or agriculture) measured at time t-h, which are contained in the $k \times 1$ vector $\mathbf{c}_{t\text{-}h}$. The $j \times 1$ vector $\mathbf{w}_t$ contains process errors, which are distributed as a multivariate normal with mean vector $\mathbf{0}$ and covariance matrix $\mathbf{Q}$.

The second part of a state-space model is the observation equation, which relates the observed data to the unobserved states:

$$\mathbf{y}_t = \mathbf{Z}\mathbf{x}_t + \mathbf{v}_t \tag{2}$$

The $i \times 1$ vector $\mathbf{y}_t$ contains the observed nutrient load or discharge in year t; i varies depending on the spatial resolution of the analysis (Text S2). The matrix $\mathbf{Z}$ maps each of the observed time series onto each of the hidden states in $\mathbf{x}_t$. By changing the structure of $\mathbf{Z}$, we evaluated statistical support for temporal synchrony of nutrient loads and discharge across different site groupings. The $i \times 1$ vector $\mathbf{v}_t$ contains the observation errors, which are distributed as a multivariate normal with mean vector $\mathbf{0}$ and covariance matrix $\mathbf{R}$. Both the observed data and the covariates were standardized to have a mean of 0 and standard deviation of 1 to facilitate model comparisons and interpretation across sites and spatial scales.

Each response variable (discharge or loads of a single nutrient) was modeled separately. For each response variable, we tested three sets of MARSS models, reflecting the three spatial scales represented in the data set: (1) the entire Mississippi-Atchafalaya Basin (hereafter "Total MARB models"), (2) four major tributary basins of the Mississippi River (Upper Mississippi, Missouri, Arkansas-Red, and Ohio-Tennessee; hereafter "Four Basins models"), and (3) 13 smaller watersheds (3 in the Upper Mississippi, 5 in the Missouri, and 5 in the Ohio-Tennessee; hereafter "Thirteen Basins models"). For the Four Basins and Thirteen Basins models, sites were either treated as independent or grouped with neighboring sites by geographic proximity or position within drainage networks (i.e., the length j of the vector $\mathbf{x}_t$ in equation (1); Text S2).

To quantify effects of climate variables on discharge and nutrient loads (Hypothesis 1A), we included covariates in MARSS models and compared model fits to the data with model fits for no-covariate models (Text S2). To test Hypothesis 2A we compared models with site-specific versus shared covariate effects for continental-scale drivers (ENSO, NAO).

For models within a given spatial scale, we evaluated the following assumptions about unmeasured environmental variation, $\mathbf{w}_t$, in equation (1): (1) independent and identically distributed, (2) independent but non-identically distributed, and (3) nonindependent but identically distributed. Models with structures of $\mathbf{Q}$ lacking covariance among sites suggest greater temporal independence among sites and would lend support for Hypothesis 2A.

Error and bias introduced by load estimation procedures may obscure relationships between climate variables and nutrient loads (Hirsch, 2014; Stenback et al., 2011). Rather than estimate observation variance for each site (e.g., the diagonal elements of $\mathbf{R}$, r_i) from the data, we derived them from the LOADEST 95% confidence intervals (USGS, 2016; Text S2). Values of r_i are reported in Table S3.

2.5. Model Fits

Models were fit to the data using maximum likelihood via an expectation-maximization algorithm run for 1000 iterations, using the "MARSS" package (Holmes et al., 2018) for the R software (R Core Team, 2015). We compared model fits using Akaike's information criterion adjusted for small sample size (AIC_c; Burnham & Anderson, 2002). A difference in AIC_c (ΔAIC_c) > 2 between models suggests moderate support for the model with the lower AIC_c; $\Delta AIC_c > 10$ shows strong support. Bias and confidence intervals around parameter estimates were calculated using parametric bootstrapping (reported in Table S7).

3. Results

3.1. Climate Effects on Discharge and Nutrients

Continental- and watershed-scale climate variables explained significant interannual variation in nutrient loads from the Mississippi River and its tributaries, whereas crop acreage did not. Effects of climate variables differed among nutrients (N and P) and nutrient forms (nitrate, ammonium), supporting Hypothesis 1A. Contrary to our expectations, continental-scale climate phenomena had no significant effects on river

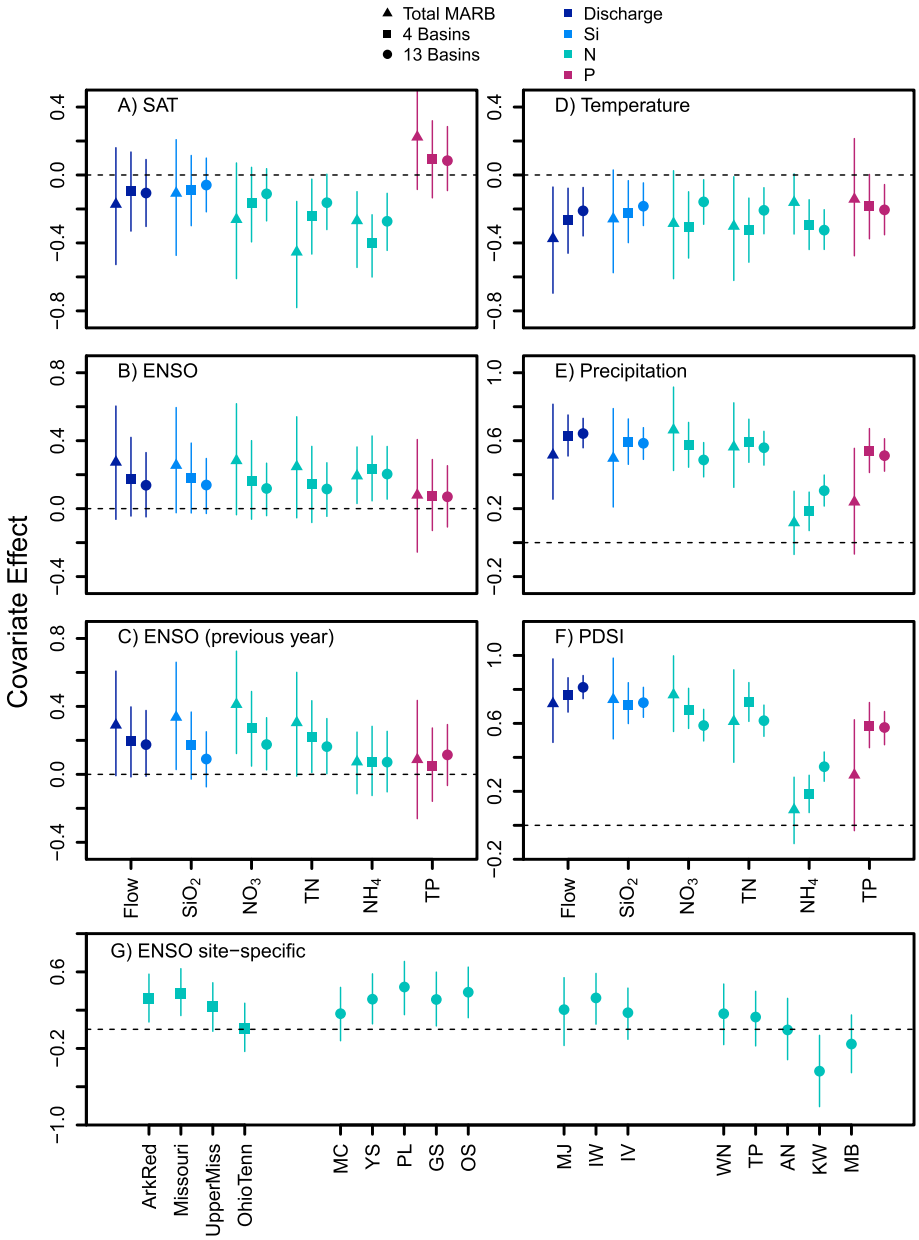

Figure 2. (a–f) Effects of continental and regional climate patterns (SAT, ENSO) on discharge and nutrient loads at the MARB scale (filled triangles), subbasin scale (filled squares), and watershed scale (filled circles). Data are standardized by mean and variance. The *y* axis extent differs among panels, but panels share the same scale. Points are maximum likelihood estimates for the effect of a climate variable on each response variable. Vertical bars represent 95% confidence intervals around parameter estimates; bars crossing the horizontal dashed line (zero) indicate lack of significance. (g) Site-specific effects of ENSO on ammonium loads. Sites are arranged along the *x* axis by longitude (west to east).

discharge or SiO_2 loads at any spatial scale. Including large-scale climate variables generally worsened model fits to the discharge, SiO_2, and P time series (e.g., increased AIC_c relative to no-covariate models; Tables S4–S6). However, we detected signals of ENSO, and land-surface temperature anomalies in N loads across multiple spatial scales (Tables S4–S6 and Figure 2). Positive temperature anomalies (SAT) were significantly related to lower total N loads from the MARB ($\Delta AIC_c > 4$; covariate effect C = −0.45 ± 0.15 (1 SE)) and its four major tributary basins ($\Delta AIC_c > 2$; −0.24 ± 0.11). Positive SAT was associated with reduced ammonium loads from the MARB ($\Delta AIC_c = 2$; −0.26 ± 0.11), the four tributaries ($\Delta AIC_c > 10$; −0.40 ± 0.09), and 13 smaller watersheds ($\Delta AIC_c > 6$; −0.27 ± 0.04; Figure 2a). High MEI values

(associated with El Niño events) were positively related to ammonium loads at all spatial scales (ΔAIC_c 2–8; effect sizes in Table S7 and Figure 2b), whereas previous-year El Niño events were related to higher nitrate loads at the subbasin and watershed scales ($\Delta AIC_c > 2$; Figure 2c). NAO had significant but variable effects on total P loads from the four subbasins (Tables S5 and S6), but was unrelated to P loads from the MARB (Table S4; results not shown in Figure 2).

Consistent with Hypothesis 1B, proximate climate variables were generally better predictors of nutrient loads and discharge than continental-scale climate variables (Tables S4–S6). Precipitation and drought severity (PDSI; positive values indicate wet conditions) had strong positive effects on discharge, total N, nitrate, and silica loads ($C > 0.5$), but smaller or insignificant effects on ammonium and total P loads (Figures 2e and 2f). Higher temperature corresponded to lower discharge and nutrient loads, although effect sizes varied among spatial scales (Table S7 and Figure 2d).

3.2. Effects of Spatial Scale on Climate-Nutrient Load Relationships

We found limited evidence for site-specific effects of continental-scale climate variables (ENSO, NAO) on nutrient loads at the same spatial scale. In all but three of 18 response variable + spatial scale combinations, models with uniform effects of climate variables had lower AIC_c than models with site-specific covariate effects, contradicting Hypothesis 2A (Tables S4–S6). The exceptions were the effect of NAO on total P loads at the subbasin scale: high NAO (current or previous year) increased total P loads from the Arkansas-Red, but had negative or neutral effects on P loads in the other subbasins. In addition, ENSO had variable effects on ammonium loads at the subbasin and watershed scales: ENSO had a positive effect on ammonium loads from the upper Mississippi, Missouri, Arkansas-Red, and smaller watersheds within the upper Mississippi and Missouri drainages, but a neutral or negative effect on ammonium loads from rivers in the Ohio-Tennessee drainage (Table S7 and Figure 2g).

Temporal dynamics of discharge and nutrient loads were largely independent among sites at the same spatial scale. Allowing time series models to follow separate state processes among sites resulted in significantly better model fits than any other grouping structure ($\Delta AIC_c > 2$; Tables S4–S6). However, there appears to be correlated "leftover" variation in discharge and nutrient loads among sites. The best process error structure for all nutrients and spatial scales included covariance among the state processes (nonzero off-diagonal terms in **Q**; Tables S4–S6).

In general, we did not observe a loss of climate signals at the MARB scale. Contrary to Hypothesis 2B, the effects of individual climate variables on discharge and nutrient loads generally remained similar in magnitude across spatial scales. For example, the positive influence of ENSO on ammonium loads remained relatively constant across all three spatial scales (effect size: 0.19–0.23; Figure 2b). For certain climate variables and nutrients, effect sizes either increased or decreased with spatial scale, although differences were not significant (95% confidence intervals overlapped with mean covariate effect estimates across scales; Figure 2). Proximate climate drivers such as precipitation had substantial influence on total P and ammonium loads from the 13 watersheds and four large tributary subbasins of the Mississippi River but no significant effects at the scale of the MARB (Figures 2e and 2f). Alternatively, the negative influence of SAT on total N loads increased in magnitude from small to large scales; at the MARB scale SAT had a larger effect on N loads than annual average temperature within the basin ($C = -0.45 \pm 0.15$ versus -0.30 ± 0.15; Figure 2a).

4. Discussion

We detected continental-scale climate signals in N loads in large river basins within the Mississippi Basin, although proximate expressions of climate are better predictors of loads. The general lack of significant large-scale climate signals (ENSO, SAT) in river discharge, SiO_2, or P load time series contrasts with the results for N loads and suggests that climate-related factors other than flow conditions can significantly influence nutrient processing and transport at continental spatial scales. This result complicates the notion that nutrient loads in the Mississippi River are a simple function of discharge, and that nutrient loss from the landscape is transport-limited (Basu et al., 2010). Climate variables differentially affected forms of nitrogen (nitrate versus ammonium), suggesting mechanisms that operate in addition to those that drive runoff or flow.

To distinguish discharge-driven temporal patterns in nutrient loads from those that arise through alternate mechanisms, we modeled discharge exactly as we modeled nutrient loads at each site and compared the magnitude and direction of climate effects on both. Climate effects on discharge were often strong but also differed substantially from the effects on nutrient loads, particularly for ammonium and total P (Figure 2). PDSI and precipitation were strongly related to discharge and silica, nitrate, and total N loads, but less related to ammonium and total P. None of the continental-scale climate variables were significantly related to discharge ($\Delta AIC_c < 2$; Tables S4–S6 and Figures 2a–2c). This does not mean that climate oscillations have no impact on discharge, but that rather that climate signals in discharge time series at the scale of the MARB can be obscured by spatial and temporal variation throughout the drainage (Rice & Emanuel, 2017; Twine et al., 2005). Despite limitations of the data used in this study that limited statistical power (Text S1), comparisons of climate effects on discharge and nutrient loads affirm that large-scale climate phenomena influence temporal patterns in nutrient loads via mechanisms operating in addition to discharge.

Nutrients are transformed and retained during riverine transport by biogeochemical processes that differentially influence various nutrient forms, although processing generally reduces loads measured at the river outlet relative to upstream landscape inputs (Alexander et al., 2000; Mulholland et al., 2008). We hypothesize that continental-scale climate variables affect nutrient forms differently through nutrient-specific biogeochemical and physical processes, both on the landscape and within the river network. Large-scale climate phenomena manifest within watersheds as proximate variables, such as precipitation and temperature, that control both river discharge (Figures 2d and 2e) and biogeochemical cycling, making it difficult to distinguish the mechanisms that link them to nutrient loads. We propose the following framework for understanding statistical climate-load relationships: (1) climate relates to loads via direct effects on runoff and discharge, (2) via biogeochemical effects on nutrient inputs (concentrations), or (3) both simultaneously (Figure S3). If climate affects a constituent load solely via runoff and discharge (scenario 1), both loads and discharge will share a similar climate response. Scenarios 2 and 3 allow for stronger linkages between loads and climate than between discharge and climate, although if effects on discharge and nutrient inputs differ in magnitude or direction, relationships may be obscured. The significant statistical relationships between various forms of N and large-scale climate phenomena (ENSO, SAT) can be explained within this framework. Specifically, we argue that at the spatial scales addressed in this study, soil moisture (redox) and temperature act as key determinants of the N transformations that link large-scale climate phenomena to nutrient loads.

Our analyses revealed a consistent inverse relationship between SAT anomaly and total N loads (-4.7×10^8 kg N per °C temperature anomaly). SAT anomaly was not significantly related to discharge ($\Delta AIC_c < 2$; Figure 2a), implying that the relationship between SAT and total N loads was not simply due to lower discharge in warm years (e.g., entirely flow-driven, scenario 1). Such a pattern might result from greater N uptake by plants under warm conditions and longer growing seasons (Groffman et al., 2018). Higher SAT also reduced ammonium loads, suggesting a potential shift in the importance of denitrification versus nitrification under warmer and drier soil conditions. Within the river network, warmer temperatures increase rates of denitrification, plant and algal uptake of N, and aerobic respiration (Song et al., 2018), which can further decrease N concentrations and loads. Higher evapotranspiration in warms years could reduce N export to rivers due to decreased subsurface flows and reduced connectivity of the river network with nutrient source areas on the landscape (Davis et al., 2014; Outram et al., 2016). While higher evapotranspiration should decrease runoff and discharge concurrently with nutrient inputs (scenario 3; Figure S3), additive effects of flow-driven and biogeochemical pathways may explain the overall stronger relationship between N loads and SAT than would be expected by flow-driven pathways alone. In contrast to total N and ammonium loads, SAT had no significant effect on nitrate loads. This finding is consistent with previous work showing that in the intensively farmed regions of the MARB, nitrate loads respond primarily to fertilizer inputs and river discharge (Raymond et al., 2012), and that there is little effect of large-scale climate phenomena on nitrate loads beyond the effect on discharge (e.g., scenario 1).

We observed a significant positive relationship between ENSO and ammonium loads ($\Delta AIC_c > 2$), whereas discharge was not significantly related ($\Delta AIC_c < 2$). Previous work has demonstrated insignificant streamflow responses to ENSO in the MARB (Munoz & Dee, 2017; Twine et al., 2005), but also that El Niño is associated with regionally coherent anomalies in soil moisture and water balance that develop at seasonal time

scales (Twine et al., 2005). Such anomalies could influence transport and transformation of N on the landscape. For example, during El Niño conditions, winters are warmer and drier, with less snow cover, across large parts of the upper Midwestern United States (Twine et al., 2005). As much as 50% of N fertilizer is applied in autumn as anhydrous ammonia in some of these regions (Gentry et al., 2009). Reduced snowpack favors soil freezing and consequently lower rates of N mineralization and nitrification (e.g., Groffman et al., 2009), including nitrification of ammonia fertilizer, and this is a plausible mechanism for higher ammonium loads observed during El Niño years (Figure 2b).

The ammonium-ENSO relationship was one of the few where watershed-specific climate effects were supported by the data (Figure 2g), and the change from positive to negative ENSO effects on ammonium loads from western to eastern drainages mirrors regional variation in spring and summer runoff and soil moisture anomalies associated with ENSO (Twine et al., 2005). We therefore speculate that the positive ENSO-ammonium relationship in the western portions of the MARB may result from reduced nitrification in soils or the river network during wet El Niño conditions (or alternatively for the eastern drainages, higher nitrification under drier conditions). Seasonal runoff and moisture anomalies associated with ENSO should decrease the residence time of water and nutrients in the soil and in the river network and reduce opportunities for biological processing. The lagged positive effect of El Niño on nitrate loads (Figure 2c) may reflect flushing from soils following dry conditions in the previous year (Loecke et al., 2017), consistent with previous findings that nitrate loads respond mainly to runoff and flow conditions (scenario 1; Raymond et al., 2012). Overall, flow-independent climatic factors appear to operate mostly on N transformations (scenario 2), many of which are biologically mediated and involve changes in oxidation state. In contrast, phosphorus does not undergo changes in oxidation state during cycling between organic and inorganic forms, although redox conditions affect sorption and desorption of P from sediments.

We expected watershed-scale variation in geomorphology, land cover (Hansen et al., 2018), and land use to diminish the detection of large-scale climate effects at scale of the MARB. However, the magnitude of climate effects on nutrient loads was relatively invariant across spatial scales (Figure 2), indicating propagation of climate signals throughout the basin. Models with covariance in the process errors (**Q** in equation (1)) among sites were supported by the data across all nutrients and spatial scales, suggesting that unmeasured climate, landscape, or anthropogenic effects on discharge and nutrient loads may promote temporal synchrony. Economic factors or governmental policies influence agricultural practices and potentially affect synchrony in nutrient loads across the MARB. For example, the 2007 U.S. ethanol mandate incentivized expanded corn production across the Midwestern United States, with expected increases in nutrient loading (Donner & Kucharik, 2008; Secchi et al., 2011). The extent to which synchrony in nutrient loads is driven by climate, policy outcomes, or their interactions is unknown and represents a critical research need in the face of increased climate variability.

Reducing nutrient runoff is a critical management goal within the MARB. Our analysis suggests that climatic factors acting through biogeochemical mechanisms may introduce uncertainty into predicted management outcomes across multiple spatial scales. One of the most consistently significant climatic factors in our analysis was SAT, which has increased in recent decades, particularly in northern midlatitudes (Ji et al., 2014). Changes in SAT or other climate phenomena will exacerbate difficulties in identifying and achieving water quality targets for the Mississippi River basin and Gulf of Mexico. Although our study was not designed to test management outcomes, our results suggest that adjustments in management goals may be required as global and regional climate continue to change.

Acknowledgments
Data used in this analysis are available online through the following U.S. government agencies: USGS, NOAA, and USDA. We thank the National Science Foundation (grant DEB-1354867) for funding the Stream Resiliency Research Coordination Network and the National Socio-Environmental Synthesis Center for hosting the working group where many of these ideas were developed. A.P.A. was partly supported by the USGS Office of Water Information. N.A.G. was partially supported by the U.S. Department of Energy's Office of Science, Biological and Environmental Research and Environmental Management Programs.

References

Alexander, R. B., Boyer, E. W., Smith, R. A., Schwarz, G. E., & Moore, R. B. (2007). The role of headwater streams in downstream water quality. *Journal of the American Water Resources Association*, *43*(1), 41–59. https://doi.org/10.1111/j.1752-1688.2007.00005.x

Alexander, R. B., Smith, R. A., & Schwarz, G. E. (2000). Effect of stream channel size on the delivery of nitrogen to the Gulf of Mexico. *Nature*, *403*(6771), 758–761. https://doi.org/10.1038/35001562

Alexander, R. B., Smith, R. A., Schwarz, G. E., Boyer, E. W., Nolan, J. V., & Brakebill, J. W. (2008). Differences in phosphorus and nitrogen delivery to the Gulf of Mexico from the Mississippi River basin. *Environmental Science and Technology*, *42*(3), 822–830. https://doi.org/10.1021/es0716103

Archfield, S. A., Hirsch, R. M., Viglione, A., & Blöschl, G. (2016). Fragmented patterns of flood change across the United States. *Geophysical Research Letters*, *43*, 10,232–10,239. https://doi.org/10.1002/2016GL070590

Aulenbach, B. T. (2013). Improving regression-model-based streamwater constituent load estimates derived from serially correlated data. *Journal of Hydrology*, *503*, 55–66. https://doi.org/10.1016/j.jhydrol.2013.09.001

Basu, N. B., Destouni, G., Jawitz, J. W., Thompson, S. E., Loukinova, N. V., Darracq, A., et al. (2010). Nutrient loads exported from managed catchments reveal emergent biogeochemical stationarity. *Geophysical Research Letters*, *37*, L14705. https://doi.org/10.1029/2010GL045168

Burnham, K. P., & Anderson, D. R. (2002). Avoiding pitfalls when using information- theoretic methods. *The Journal of Wildlife Management*, *66*(3), 912–918. Retrieved from http://www.jstor.org/stable/3803155

Chen, J., & Kumar, P. (2002). Role of terrestrial hydrologic memory in modulating ENSO impacts in North America. *Journal of Climate*, *15*(24), 3569–3585. https://doi.org/10.1175/1520-0442(2003)015<3569:ROTHMI>2.0.CO;2

Dale, V. H., Wright, D., Kling, C. L., Boynton, W., Meyer, J. L., Mankin, K., et al. (2010). In B. N. Anderson, R. W. Howarth, & L. R. Walker (Eds.), *Hypoxia in the Northern Gulf of Mexico*. New York: Springer. https://doi.org/10.1007/978-0-387-89686-1_1

Davis, C. A., Ward, A. S., Burgin, A. J., Loecke, T. D., Riveros-Iregui, D. A., Schnoebelen, D. J., et al. (2014). Antecedent moisture controls on stream nitrate flux in an agricultural watershed. *Journal of Environmental Quality*, *43*(4), 1494. https://doi.org/10.2134/jeq2013.11.0438

Donner, S. D., & Kucharik, C. J. (2008). Corn-based ethanol production compromises goal of reducing nitrogen export by the Mississippi River. *Proceedings of the National Academy of Sciences*, *105*(11), 4513–4518. https://doi.org/10.1073/pnas.0708300105

Donner, S. D., & Scavia, D. (2007). How climate controls the flux of nitrogen by the Mississippi River and the development of hypoxia in the Gulf of Mexico. *Limnology and Oceanography*, *52*(2), 856–861. https://doi.org/10.4319/lo.2007.52.2.0856

ESRI (2016). *ArcGIS Desktop*. Redlands, CA: Environmental Systems Research Institute.

Frans, C., Istanbulluoglu, E., Mishra, V., Munoz-Arriola, F., & Lettenmaier, D. P. (2013). Are climatic or land cover changes the dominant cause of runoff trends in the Upper Mississippi River basin? *Geophysical Research Letters*, *40*, 1104–1110. https://doi.org/10.1002/grl.50262

Gentry, L. E., David, M. B., Below, F. E., Royer, T. V., & McIsaac, G. F. (2009). Nitrogen mass balance of a tile-drained agricultural watershed in east-central Illinois. *Journal of Environmental Quality*, *38*(5), 1841. https://doi.org/10.2134/jeq2008.0406

Groffman, P. M., Driscoll, C. T., Durán, J., Campbell, J. L., Christenson, L. M., Fahey, T. J., et al. (2018). Nitrogen oligotrophication in northern hardwood forests. *Biogeochemistry*, *141*(3), 523–539. https://doi.org/10.1007/s10533-018-0445-y

Groffman, P. M., Hardy, J. P., Fisk, M. C., Fahey, T. J., & Driscoll, C. T. (2009). Climate variation and soil carbon and nitrogen cycling processes in a northern hardwood forest. *Ecosystems*, *12*(6), 927–943. https://doi.org/10.1007/s10021-009-9268-y

Hansen, A. T., Dolph, C. L., Foufoula-Georgiou, E., & Finlay, J. C. (2018). Contribution of wetlands to nitrate removal at the watershed scale. *Nature Geoscience*, *11*(2), 127–132. https://doi.org/10.1038/s41561-017-0056-6

Hansen, J., Ruedy, R., Sato, M., Imhoff, M., Lawrence, W., Easterling, D., et al. (2001). A closer look at United States and global surface temperature change. *Journal of Geophysical Research*, *106*(D20), 23,947–23,963. https://doi.org/10.1029/2001JD000354

Hirsch, R. M. (2014). Large biases in regression-based constituent flux estimates: causes and diagnostic tools. *Journal of the American Water Resources Association*, *50*(6), 1401–1424. https://doi.org/10.1111/jawr.12195

Holmes, E. E., Ward, E. J., & Scheuerell, M. D. (2018). *Analysis of Multivariate Time-Series Using the MARSS Package*. Seattle, WA: DOC-NOAA-NMFS-NWC. Retrieved from http://cran.r-project.org/web/packages/MARSS/vignettes/UserGuide.pdf

Hurrell North Atlantic Oscillation (NAO) Index (PC-Based) (2016). Retrieved from https://climatedataguide.ucar.edu/climate-data/hurrell-north-atlantic-oscillation-nao-index-pc-based

Ji, F., Wu, Z., Huang, J., & Chassignet, E. P. (2014). Evolution of land surface air temperature trend. *Nature Climate Change*, *4*(6), 462–466. https://doi.org/10.1038/nclimate2223

Jorgensen, J. C., Ward, E. J., Scheuerell, M. D., & Zabel, R. W. (2016). Assessing spatial covariance among time series of abundance. *Ecology and Evolution*, *6*(8), 2472–2485. https://doi.org/10.1002/ece3.2031

Lee, C. J., Murphy, C. J., Crawford, C. G., & Deacon, J. R. (2017). Methods for computing water-quality loads at sites in the U.S. Geological Survey National Water Quality Network. *U.S. Geological Survey Open-File Report 2017–1120*. https://doi.org/https://doi.org/10.3133/ofr20171120

Loecke, T. D., Burgin, A. J., Riveros-Iregui, D. A., Ward, A. S., Thomas, S. A., Davis, C. A., & Clair, M. A. S. (2017). Weather whiplash in agricultural regions drives deterioration of water quality. *Biogeochemistry*, *133*(1), 7–15. https://doi.org/10.1007/s10533-017-0315-z

McCluney, K. E., Poff, N. L., Palmer, M. A., Thorp, J. H., Poole, G. C., Williams, B. S., et al. (2014). Riverine macrosystems ecology: Sensitivity, resistance, and resilience of whole river basins with human alterations. *Frontiers in Ecology and the Environment*, *12*(1), 48–58. https://doi.org/10.1890/120367

Mulholland, P. J., Helton, A. M., Poole, G. C., Hall, R. O., Hamilton, S. K., Peterson, B. J., et al. (2008). Stream denitrification across biomes and its response to anthropogenic nitrate loading. *Nature*, *452*(7184), 202–205. https://doi.org/10.1038/nature06686

Munoz, S. E., & Dee, S. G. (2017). El Niño increases the risk of lower Mississippi River flooding. *Scientific Reports*, *7*(1), 1–7. https://doi.org/10.1038/s41598-017-01919-6

NASA (2016). Global mean estimates based on land-surface air temperature anomalies only (meteorological station data, dTs): Zonal annual means. Retrieved June 20, 2017, from https://data.giss.nasa.gov/gistemp/tabledata_v3/ZonAnn.Ts.txt

NOAA (2016a). Divisional temperature-precipitation-drought. Retrieved from ftp://ftp.ncdc.noaa.gov/pub/data/cirs/climdiv/

NOAA (2016b). MEI index. Retrieved from http://www.esrl.noaa.gov/psd/enso/mei/table.html

Ohlberger, J., Scheuerell, M. D., & Schindler, D. E. (2016). Population coherence and environmental impacts across spatial scales: A case study of Chinook salmon. *Ecosphere*, *7*(4), 1–14. https://doi.org/10.1002/ecs2.1333

Outram, F. N., Cooper, R. J., Sünnenberg, G., Hiscock, K. M., & Lovett, A. A. (2016). Antecedent conditions, hydrological connectivity and anthropogenic inputs: Factors affecting nitrate and phosphorus transfers to agricultural headwater streams. *Science of the Total Environment*, *545–546*, 184–199. https://doi.org/10.1016/j.scitotenv.2015.12.025

R Core Team (2015). R: A language and environment for statistical computing (R Foundation for Statistical Computing Vienna). Retrieved from www.R-project.org/

Rabalais, N. N., Turner, R. E., & Wiseman, W. J. (2002). Gulf of Mexico hypoxia, a.k.a. "the dead zone.". *Annual Review of Ecology and Systematics*, *33*(1), 235–263. https://doi.org/10.1146/annurev.ecolsys.33.010802.150513

Räsänen, T. A., Lehr, C., Mellin, I., Ward, P. J., & Kummu, M. (2013). Palaeoclimatological perspective on river basin hydrometeorology: Case of the Mekong Basin. *Hydrology and Earth System Sciences*, *17*(5), 2069–2081. https://doi.org/10.5194/hess-17-2069-2013

Raymond, P. A., David, M. B., & Saiers, J. E. (2012). The impact of fertilization and hydrology on nitrate fluxes from Mississippi watersheds. *Current Opinion in Environmental Sustainability*, *4*(2), 212–218. https://doi.org/10.1016/j.cosust.2012.04.001

Rice, J. S., & Emanuel, R. E. (2017). How are streamflow responses to the El Nino Southern Oscillation affected by watershed characteristics? *Water Resources Research*, *53*, 4393–4406. https://doi.org/10.1002/2016WR020097

Royer, T. V., David, M. B., & Gentry, L. E. (2006). Timing of riverine export of nitrate and phosphorus from agricultural watersheds in Illinois: Implications for reducing nutrient loading to the Mississippi River. *Environmental Science and Technology*, *40*(13), 4126–4131. https://doi.org/10.1021/es052573n

Runkel, R. L., Crawford, C. G., & Cohn, T. A. (2004). Load estimator (LOADEST)—A FORTRAN program for estimating constituent loads in streams and rivers. In *U.S. Geological Survey Techniques and Methods Book 4*. (Chapter A5, pp. 1–55). Reston, VA: U.S. Department of the Interior, U.S. Geological Survey.

Secchi, S., Gassman, P. W., Jha, M., Kurkalova, L., & Kling, C. L. (2011). Potential water quality changes due to corn expansion in the Upper Mississippi River basin. *Ecological Applications*, *21*(4), 1068–1084. https://doi.org/10.1890/09-0619.1

Sinha, E., Michalak, A., & Balaji, V. (2017). Eutrophication will increase during the 21st century as a result of precipitation changes. *Science*, *357*(6349), 405–408. https://doi.org/10.1126/science.aan2409

Sinha, E., & Michalak, A. M. (2016). Precipitation dominates interannual variability of riverine nitrogen loading across the continental United States. *Environmental Science and Technology*, *50*(23), 12,874–12,884. https://doi.org/10.1021/acs.est.6b04455

Song, C., Dodds, W. K., Rüegg, J., Argerich, A., Baker, C. L., Bowden, W. B., et al. (2018). Productivity in streams due to climate warming. *Nature Geoscience*, *11*(June), 415–420. https://doi.org/10.1038/s41561-018-0125-5

Stenback, G. A., Crumpton, W. G., Schilling, K. E., & Helmers, M. J. (2011). Rating curve estimation of nutrient loads in Iowa rivers. *Journal of Hydrology*, *396*(1–2), 158–169. https://doi.org/10.1016/j.jhydrol.2010.11.006

Turner, R. E., Rabalais, N. N., & Justić, D. (2012). Predicting summer hypoxia in the northern Gulf of Mexico: Redux. *Marine Pollution Bulletin*, *64*(2), 319–324. https://doi.org/10.1016/j.marpolbul.2011.11.008

Twine, T. E., Kucharik, C. J., & Foley, J. A. (2005). Effects of El Nino-Southern Oscillation on the climate, water balance, and streamflow of the Mississippi River basin. *Journal of Climate*, *18*(22), 4840–4861. https://doi.org/10.1175/JCLI3566.1

USDA (2016). National Agricultural Statistics Service. Retrieved from https://quickstats.nass.usda.gov/

USGS (2009). National elevation dataset. Retrieved from http://nationalmap.gov

USGS (2016). Streamflow and nutrient flux of the Mississippi-Atchafalaya River Basin and subbasins through water year 2016. Retrieved from https://toxics.usgs.gov/hypoxia/mississippi/flux_ests/index.html

Vose, R. S., Applequist, S., Squires, M., Durre, I., Menne, C. J., Williams, C. N., et al. (2014). Improved historical temperature and precipitation time series for U.S. climate divisions. *Journal of Applied Meteorology and Climatology*, *53*(5), 1232–1251. https://doi.org/10.1175/JAMC-D-13-0248.1